

## Acknowledgments

This study was supported by funding from Spectrum Astro IR&D, with special encouragement from Stanley Dubyn. The author thanks F. L. Markley of NASA Goddard Space Flight Center, Robert Bauer of Bauer Engineering, and Carl Hubert of Hubert Astronautics for helpful comments and suggestions.

## References

- <sup>1</sup>King, B. G., and Woolley, R. P., "Modeling, Tuning, and Effectiveness of Partially-Filled Ring Nutation Dampers," *Advances in the Astronautical Sciences*, Vol. 57, edited by R. D. Culp, E. J. Bauman, and C. A. Cullian, American Astronautical Society, Springfield, VA, 1985, pp. 431–452.
- <sup>2</sup>Constantinescu, V. N., *Laminar Viscous Flow*, Springer-Verlag, New York, 1995, pp. 193–195.
- <sup>3</sup>Hubert, C., and Swanson, D., "Surface Tension Lockup in the IMAGE Nutation Damper—Anomaly and Recovery," *2001 Flight Mechanics Symposium*, edited by J. P. Lynch, NASA Goddard Space Flight Center, Greenbelt, MD, 2001, p. 527.
- <sup>4</sup>Arfken, G., *Mathematical Methods for Physicists*, Academic Press, Boston, 1985, pp. 573–584.
- <sup>5</sup>Beyer, W. H., *CRC Standard Mathematical Tables*, CRC Press, Boca Raton, FL, 1984, pp. 349–351.
- <sup>6</sup>Gradshteyn, I. S., and Ryzhik, I. M., *Table of Integrals, Series, and Products*, Academic Press, Boston, 1980, pp. 951–954.
- <sup>7</sup>Kreyszig, E., *Advanced Engineering Mathematics*, Wiley, New York, 1993, pp. 225–231.
- <sup>8</sup>Kaplan, M. H., *Modern Spacecraft Dynamics and Control*, Wiley, New York, 1976, pp. 131–139.
- <sup>9</sup>Bhuta, P. G., and Koval, L. R., "A Viscous Ring Damper for a Freely Precessing Satellite," *International Journal of the Mechanical Sciences*, Vol. 8, 1966, pp. 383–394.

# Gravity-Turn Descent from Low Circular Orbit Conditions

Colin R. McInnes\*

University of Glasgow,

Glasgow, Scotland G12 8QQ, United Kingdom

## Introduction

**G**RAVITY-TURN descent to the surface of a planetary or small solar system body has been investigated for many years and, indeed, has been used for both lunar and Mars descent vehicles.<sup>1–5</sup> Such a descent profile requires that the vehicle thrust vector is oriented opposite to the instantaneous velocity vector along the entire descent trajectory. This requirement can be achieved with knowledge of the vehicle velocity vector from an inertial measurement unit and an attitude control system that can maintain the thrust vector antiparallel to the instantaneous velocity vector.<sup>1</sup> For pure gravity-turn descent, the steering law is, therefore, relatively easy to implement in practice, although the descent may be modified at the terminal phase for surface hazard avoidance. An important benefit of gravity-turn descent is that the landing is assured to be vertical, and the steering law is close to fuel optimum.<sup>3</sup>

The equations of motion for gravity-turn descent can be solved in closed form for a fixed thrust-to-weight ratio, assuming that a constant, vertical gravitational acceleration is the only other force acting on the descent vehicle.<sup>1</sup> The latter approximation limits the validity of the solutions to regimes where the descent vehicle velocity is small relative to the local circular orbit velocity because centripetal

forces are ignored. The closed-form solutions can, therefore, only be used to describe terminal descent, when the vehicle has braked from circular orbit velocity and is close to the planetary surface. In this Note, it will be demonstrated that the equations of motion for gravity-turn descent can, in fact, be solved in closed form if centripetal forces are retained, but gravity is assumed to be constant in magnitude. Because the descent will normally begin from a low circular parking orbit, these assumptions appear reasonable. New solutions are found that allow a full representation of the descent vehicle motion from circular orbit conditions down to the final landing event.

## Classical Gravity-Turn Solutions

The general equations of motion for the descent vehicle can be written in normal-tangential coordinates, with the vehicle thrust-induced acceleration written as  $Ng_0$ , where  $N$  is the thrust-to-weight ratio and  $g_0$  is the gravitational acceleration at the planetary surface, as shown in Fig. 1. For a planetary or small solar system body of radius  $R$ , the equations of motion may be written as

$$\frac{dv}{dt} = g_0 \frac{R^2}{(R+h)^2} \cos \psi - Ng_0 \quad (1a)$$

$$v \frac{d\psi}{dt} = \left\{ \frac{v^2}{R+h} - g_0 \frac{R^2}{(R+h)^2} \right\} \sin \psi \quad (1b)$$

$$\frac{dh}{dt} = -v \cos \psi \quad (1c)$$

where  $v$  is the vehicle velocity,  $\psi$  is the pitch angle of the vehicle velocity vector relative to the local vertical, and  $h$  is the vehicle altitude above the planetary surface. The classical gravity-turn solutions can be obtained by assuming the descent takes place over a plane so that  $R \rightarrow \infty$ . In this limit, the equations of motion reduce to

$$\frac{dv}{dt} = g_0 \cos \psi - Ng_0 \quad (2a)$$

$$v \frac{d\psi}{dt} = -g_0 \sin \psi \quad (2b)$$

These reduced equations may now be used to form a single, separable differential equation with  $\psi$  as the independent variable, such that

$$\frac{1}{v} \frac{dv}{d\psi} + \cot \psi - N \operatorname{cosec} \psi = 0 \quad (3)$$

This equation can now be directly integrated to obtain the descent vehicle velocity  $v$  as a function of the velocity vector pitch angle  $\psi$  as<sup>1</sup>

$$v(\psi) = v_0 \left\{ \frac{\sin \psi_0}{\sin \psi} \right\} \left\{ \frac{\tan(\psi/2)}{\tan(\psi_0/2)} \right\}^N \quad (4)$$

A typical descent trajectory in the  $v$ - $\psi$  plane is shown in Fig. 2 for a thrust-to-weight ratio  $N = 2$ , with a numerically integrated solution of Eq. (1) provided for comparison. The descent begins from circular orbit conditions. It can be seen that this closed-form solution

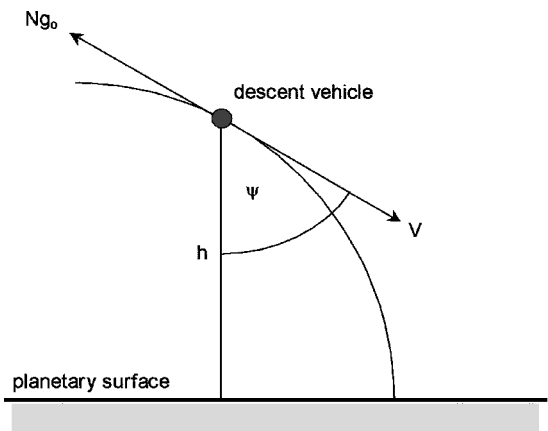


Fig. 1 Schematic of gravity-turn descent.

Received 4 December 2001; revision received 1 April 2002; accepted for publication 29 June 2002. Copyright © 2002 by the American Institute of Aeronautics and Astronautics, Inc. All rights reserved. Copies of this paper may be made for personal or internal use, on condition that the copier pay the \$10.00 per-copy fee to the Copyright Clearance Center, Inc., 222 Rosewood Drive, Danvers, MA 01923; include the code 0731-5090/03 \$10.00 in correspondence with the CCC.

\*Professor, Department of Aerospace Engineering; colinmc@aero.gla.ac.uk.

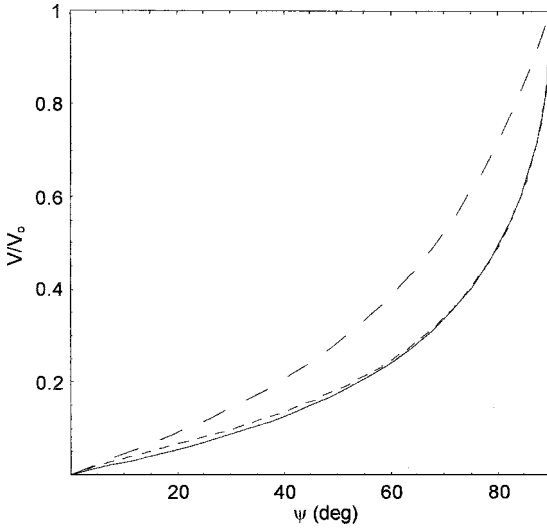


Fig. 2 Velocity-pitch angle profile: ---, numerical integration; - · -, classical gravity-turn solution; and —, extended gravity-turn solution, with  $N = 2$  and  $\lambda = 1$ .

is only a reasonable approximation to the true descent trajectory at the terminal phase of the descent, as expected. If the descent velocity is of the same order as the circular orbit velocity, the solution is extremely poor.

### Extended Gravity-Turn Solutions

The classical gravity turn solution can now be significantly improved by retaining the centripetal acceleration term in the equations of motion. Here, the earlier assumption  $R \rightarrow \infty$  is replaced with the assumption  $h/R \ll 1$ , so that the equations of motion now reduce to

$$\frac{dv}{dt} = g_0 \cos \psi - N g_0 \quad (5a)$$

$$v \frac{d\psi}{dt} = \left\{ \frac{v^2}{R} - g_0 \right\} \sin \psi \quad (5b)$$

With this approximation, there is no limitation on the descent vehicle velocity magnitude. The only requirement is that the descent must take place close to the planetary surface to ensure that the magnitude of the gravitational force is constant and that the centripetal force loses its functional dependence on altitude. For a planetary or small-body descent from a low parking orbit, these are reasonable, practical approximations to make.

The new reduced equations may again be used to form a single, separable differential equation with  $\psi$  as the independent variable, such that

$$\frac{1}{v} \left\{ 1 - \frac{v^2}{v_c^2} \right\} \frac{dv}{d\psi} + \cot \psi - N \operatorname{cosec} \psi = 0 \quad (6)$$

where  $v_c = \sqrt{g_0 R}$  is a measure of the circular orbit speed. It can be seen that Eq. (6) is similar to the classical gravity-turn equation, but with an additional term premultiplying the derivative. Again, for the classical gravity-turn problem,  $v \ll v_c$ , so that Eq. (3) is recovered. For descent from circular orbit conditions  $v \sim v_c$ , so that the centripetal acceleration is of the same order as the gravitational acceleration. In this case, Eq. (6) can still be integrated because it remains separable. The resulting solution may be written as

$$\log(v/v_0) - (1/2v_c^2)(v^2 - v_0^2) = \log G(\psi) \quad (7)$$

where

$$G(\psi) = \left\{ \frac{\sin \psi_0}{\sin \psi} \right\} \left\{ \frac{\tan(\psi/2)}{\tan(\psi_0/2)} \right\}^N \quad (8)$$

It can be seen that the centripetal acceleration has added a quadratic term to the classical gravity-turn solution of Eq. (4), which can be neglected if  $v \ll v_c$ . To proceed, a more useful way to write Eq. (7) is

$$\tilde{v} \exp(-\lambda \tilde{v}^2) = \exp(-\lambda) G^2(\psi) \quad (9)$$

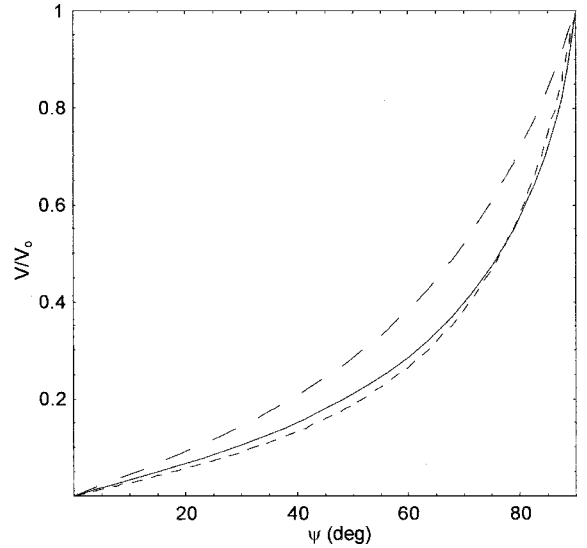


Fig. 3 Velocity-pitch angle profile: ---, first-order solution; - · -, classical gravity-turn solution; and —, extended gravity-turn solution, with  $N = 2$  and  $\lambda = 0.64$ .

where  $\tilde{v} = v/v_0$  is the nondimensional descent vehicle velocity and  $\lambda = (v_0/v_c)^2$  is a measure of the effect of the centripetal acceleration. Again, the classical gravity-turn solution is recovered in the limit  $\lambda \rightarrow 0$ . For  $\lambda \sim 1$ , the solution can be written in explicit form using the Lambert  $W$  function,<sup>6</sup> the solution to which is implemented in symbolic mathematics packages as the ProductLog function. This function is defined such that ProductLog[ $z$ ] returns the principal solution of  $z = W e^W$ , with ProductLog[ $z$ ] being real if  $z > -1/e$ , and can be viewed as an extension of the usual logarithm function. The function also satisfies the differential equation  $dW/dz + W/z(1+W)$ . By the use of this function, it can be shown that Eq. (9) provides the normalized velocity as

$$\tilde{v}(\psi) = (i/\sqrt{\lambda}) \{ W[-\lambda \exp(-\lambda) G^2(\psi)] \}^{\frac{1}{2}} \quad (10)$$

where  $i = \sqrt{-1}$  and the positive branch solution has been selected. A comparison of this new solution with the classical gravity-turn solution, and a numerically integrated solution to the full equations of motion, is shown in Fig. 2 for a thrust-to-weight ratio  $N = 2$  and  $\lambda = 1$ . It can be seen that the new solution provides an extremely good match to the exact numerical solution, with the small discrepancy at the end of the descent being due to the assumption that the gravitational force is constant in magnitude. The new solution still retains the desirable property that  $\tilde{v} \rightarrow 0$  as  $\psi \rightarrow 0$ , as can be shown analytically.

To avoid the use of special functions, Eq. (9) can be expanded in powers of  $\lambda$  to provide a correction to the classical gravity-turn solution for which  $\lambda = 0$ . In particular, Eq. (9) may be written as

$$\tilde{v}^2 = G^2(\psi) \left\{ 1 + (\tilde{v}^2 - 1)\lambda + \frac{1}{2}(\tilde{v}^2 - 1)\lambda^2 + \dots \right\} \quad (11)$$

Therefore, when only the first-order term is retained, the classical gravity-turn solution can be modified to obtain

$$\tilde{v} = G(\psi) \left\{ \frac{1 - \lambda}{1 - \lambda G(\psi)} \right\}^{\frac{1}{2}}, \quad \lambda \neq 1 \quad (12)$$

which still satisfies the boundary conditions  $\tilde{v} \rightarrow 1$  as  $\psi \rightarrow \psi_0$  and  $\tilde{v} \rightarrow 0$  as  $\psi \rightarrow 0$ . Again, a comparison of this first-order solution with the classical gravity-turn solution, and the new solution to the full equations of motion [Eq. (10)], is shown in Fig. 3 for a thrust-to-weight ratio  $N = 2$  and  $\lambda = 0.64$  ( $\tilde{v}_0 \sim 0.8v_c$ ). It can be seen that the first-order solution provides a good representation of the descent trajectory for a moderate value of  $\lambda$ , although the solution does break down in the limit as  $\lambda \rightarrow 1$ .

### Conclusions

The classical gravity-turn descent problem has been extended to allow an accurate representation of descent from circular orbit conditions. This greatly extends the domain of validity of the classical

gravity-turn solution from low-velocity terminal descent to complete descent from a low parking orbit. Although the solution to the modified gravity-turn problem can be obtained exactly as a special function, a first-order correction to the classical gravity-turn solution can extend its validity to a larger range of descent velocities. The availability of the descent vehicle velocity as a function of the velocity pitch angle could, in principle, be used to reduce the computational burden on real-time guidance algorithms for future lander missions.

### Acknowledgment

This work was performed with support from the Leverhulme Trust.

### References

- <sup>1</sup>Cheng, R. K., "Lunar Terminal Guidance," *Lunar Missions and Exploration*, edited by C. T. Leondes and R. W. Vance, Univ. of California Engineering and Physical Sciences Extension Series, Wiley, New York, 1964, pp. 308–355.
- <sup>2</sup>Citron, S. J., Dunin, S. E., and Messinger, H. F., "A Terminal Guidance Technique for Lunar Landing," *AIAA Journal*, Vol. 2, No. 3, 1964, pp. 503–509.
- <sup>3</sup>Cheng, R. K., Meredith, C. M., and Conrad, D. A., "Design Considerations for Surveyor Guidance," *Journal of Spacecraft and Rockets*, Vol. 3, No. 11, 1966, pp. 1569–1576.
- <sup>4</sup>Euler, E. A., Adams, G. L., and Hopper, F. W., "Design and Reconstruction of the Viking Lander Descent Trajectories," *Journal of Guidance, Control, and Dynamics*, Vol. 1, No. 5, 1978, pp. 372–78.
- <sup>5</sup>McInnes, C. R., "Gravity-Turn Descent with Quadratic Air Drag," *Journal of Guidance, Control, and Dynamics*, Vol. 20, No. 2, 1997, pp. 393, 394.
- <sup>6</sup>Corless, R. M., Gonnet, G. H., Hare, D. E. G., Jeffrey, D. J., and Knuth, D. E., "On the Lambert W Function," *Advances in Computational Mathematics*, Vol. 5, 1996, pp. 329–359.

## Riccati Dichotomic Basis Method for Solving Hypersensitive Optimal Control Problems

Anil V. Rao\*

Charles Stark Draper Laboratory, Inc.,  
Cambridge, Massachusetts 01239

### Introduction

**M**ANY optimal control problems and their associated Hamiltonian boundary-value problems (HBVPs) that arise from the first-order optimality conditions are hypersensitive.<sup>1–3</sup> An optimal control problem is hypersensitive if the time interval of interest is long relative to the rate of expansion and contraction of the Hamiltonian dynamics in certain directions in a neighborhood of the optimal solution. Hypersensitive HBVPs are a challenge to solve numerically because they suffer from ill-conditioning as a result of extreme sensitivity to unknown boundary conditions. When the rates are fast in all directions, the HBVP and the optimal control problem are called completely hypersensitive; when the rates are fast only in certain some directions, the HBVP and the optimal control problem are called partially hypersensitive. In this Note we are interested in completely hypersensitive HBVPs.

The solution to a completely hypersensitive HBVP can be approximated by concatenating an initial boundary-layer segment, an equilibrium segment, and a terminal boundary-layer segment.<sup>1–3</sup>

Received 11 June 2002; revision received 16 August 2002; accepted for publication 20 August 2002. Copyright © 2002 by Anil V. Rao and The Charles Stark Draper Laboratory, Inc. Published by the American Institute of Aeronautics and Astronautics, Inc., with permission. Copies of this paper may be made for personal or internal use, on condition that the copier pay the \$10.00 per-copy fee to the Copyright Clearance Center, Inc., 222 Rosewood Drive, Danvers, MA 01923; include the code 0731-5090/03 \$10.00 in correspondence with the CCC.

\*Senior Member of the Technical Staff, 555 Technology Square, Mail Stop 70; arao@draper.com. Member AIAA.

The initial boundary-layer segment has no unstable component in forward time, whereas the terminal boundary-layer segment has no unstable component in backward time. This three-segment approximation improves as the time interval of interest increases.

Recently, a new approach has been developed to solving completely hypersensitive nonlinear HBVPs arising in optimal control.<sup>1–3</sup> This method is inspired by the computational singular perturbation methodology for stiff initial-value problems.<sup>4,5</sup> The method uses a dichotomic basis to decompose the nonlinear Hamiltonian vector field into its contracting and expanding components, thus allowing the missing conditions required to specify the initial and terminal boundary-layer segments to be determined from partial equilibrium conditions. The key feature of the method is that, by using a dichotomic basis, the unstable (expanding) component of the Hamiltonian vector field can be eliminated, thereby removing the hypersensitivity. The solution of the initial boundary-layer segment is then found by integrating the stable component of the Hamiltonian vector field forward in time. Similarly, the solution of the terminal boundary-layer segment is found by integrating the unstable component of the Hamiltonian vector field backward in time.

In previous work on hypersensitive optimal control problems, the properties of a dichotomic basis were described, but no such basis had actually been found. Consequently, it was necessary to determine a solution to a completely hypersensitive HBVP using an approximate dichotomic basis. Although this method has shown some success, it can potentially fail because a sufficiently good approximate dichotomic basis can be difficult to determine. The major advancements of this research over previous work in the area of completely hypersensitive optimal control<sup>1–3</sup> are as follows: 1) the derivation of a dichotomic basis along the solution of a completely hypersensitive HBVP in the initial boundary layer and 2) the development of a successive approximation procedure to compute this dichotomic basis and the initial boundary-layer solution. The dichotomic basis described in this Note is found by solving a Riccati differential equation. The need for a successive approximation procedure arises because the solution in the initial boundary layer is not known a priori. The successive approximation procedure is illustrated on a problem in supersonic aircraft flight, and its range of applicability is assessed.

### Hamiltonian Boundary-Value Problem

In this Note we are interested in the following class of optimal control problems. Find the piecewise continuous control  $u(t) \in \mathbb{R}^m$  on  $t \in [0, t_f]$  that minimizes the scalar cost functional

$$J = \int_0^{t_f} \mathcal{L}[x, u] dt \quad (1)$$

subject to the differential constraint

$$\dot{x} = f(x, u) \quad (2)$$

and boundary conditions

$$x(0) = x_0, \quad x(t_f) = x_f \quad (3)$$

where  $x(t) \in \mathbb{R}^n$  is the state.

The first-order necessary conditions for optimality lead to a HBVP for the extremal trajectories. The HBVP is composed of the Hamiltonian differential equations

$$\dot{x} = \left[ \frac{\partial H^*}{\partial \lambda} \right]^T \equiv [H_\lambda^*]^T, \quad \dot{\lambda} = - \left[ \frac{\partial H^*}{\partial x} \right]^T \equiv -[H_x^*]^T \quad (4)$$

where  $\lambda(t) \in \mathbb{R}^n$  is the adjoint and  $H^*(x, \lambda) = \mathcal{L}[x, u^*(x, \lambda)] + \lambda^T f[x, u^*(x, \lambda)]$  is the Hamiltonian evaluated at the optimal control  $u^*(x, \lambda) = \arg \min_u H(x, \lambda, u)$ . Points  $p = (x, \lambda)$  lie in the  $2n$ -dimensional Hamiltonian phase space or, more simply, the phase space. Because  $J$  and  $f(x, u)$  do not depend explicitly on time,  $H^*$  is constant along trajectories of Eq. (4). We use  $\dot{p} = G(p)$  as an alternate expression for the Hamiltonian system in Eq. (4) and refer to  $G(p)$  as the Hamiltonian vector field, where  $G(p)$  is assumed to be continuously differentiable.